Resolution of the long-standing overprediction of the resonance to intercombination line-intensity ratio in mid-*Z* neonlike ions

Kevin B. Fournier and Stephanie B. Hansen
Lawrence Livermore National Laboratory, P.O. Box 808, L-473, Livermore, California 94550, USA
(Received 15 September 2004; published 31 January 2005)

The Ne-like resonance $2p^6\ ^1S$-$2p^5 3d\ ^1P$ ($3C$) to intercombination $2p^6\ ^1S$-$2p^5 3d\ ^3D$ ($3D$) line-intensity ratio, $R(3C/3D)$, has been extensively studied through high-accuracy measurements and calculations of atomic structure and collision cross sections. However, even state-of-the-art relativistic multiconfiguration atomic-physics codes generally predict values of $R(3C/3D)$ that are significantly larger than those observed in coronal-density experiments. In this paper, predictions of $R(3C/3D)$ across the Ne-like isoelectronic sequence from chromium to silver are brought into agreement with coronal-density experimental measurements in two steps: first by including a semiempirical correction in the collisional atomic data due to configuration-interaction effects, and next by including the effects of cascades on the upper level populations. The configuration-interaction correction is inspired by the observation that nearly all data-production codes fail to predict $R(3C/3D)$ correctly and is justified theoretically by a careful analysis of configuration-interaction contributions to level energies. The dependence of $R(3C/3D)$ with electron density and its agreement with moderate-density measurements are shown. A brief description of the application of our technique to line ratios in He- and Ni-like x-ray spectra is also given.

DOI: 10.1103/PhysRevA.71.012717 PACS number(s): 34.80.Kw, 32.70.Fw, 32.30.Rj

I. INTRODUCTION

With its closed-shell ground configuration, the Ne-like ion is stable against ionization across a relatively broad range of temperatures. Spectra from Ne-like ions, with only a few strong and well-resolved emission lines, are workhorse spectroscopic diagnostic probes of plasma temperature and density conditions in both astrophysical [1–9] and laboratory plasmas [10–14]. The Ne-like spectrum has been extensively studied through experimental measurements and theoretical calculations, and yet there is persistent disagreement between the experimental and theoretical values of the $3C/3D$ Ne-like line-intensity ratio, $R(3C/3D)$ [$3c$: $2s^2 2p^6\ ^1S_0$-$2s^2 2p^5 3d\ ^1P_1$ (LS-coupling) or $(2p_{1/2}, 3d_{3/2})_1$ (jj-coupling) and $3D$: $2s^2 2p^6\ ^1S_0$-$2s^2 2p^5 3d\ ^3D_1$ or $(2p_{3/2}, 3d_{5/2})_1$]. In 2003, Beiersdorfer [15] pointed out that calculations have overpredicted $R(3C/3D)$ in Fe XVII since the 1980s. This failure of theoretical atomic calculations to predict correctly a relatively simple ratio in the Fe XVII spectrum has cast doubt on the absolute accuracy of calculated atomic data and has given rise to energetic debate about the role of physical processes such as resonance scattering of line radiation in the solar corona [5,16–18]. Recent high-precision electron beam ion-trap (EBIT) measurements of the isolated $3C$ and $3D$ lines [19,20] have clarified the roles of line blends and resonance scattering in the observed stellar-coronae Fe XVII ratios. The EBIT experiments have shown that for observations over a range of temperatures, Fe XVI satellites give a spurious enhancement of the $3D$ intensity, and remove any question about optical depth from the interpretation of the $3C$ resonance line intensity from astrophysical sources [20]. However, modern atomic physics codes (e.g., [21–23], and many others to be discussed below) still cannot correctly predict $R(3C/3D)$ for Fe XVII. One exception, discussed below, are the Fe XVII calculations of Chen and Pradhan [24,25]. Further measurements [26,27] from low-density plasmas have shown that the theoretical overprediction of $R(3C/3D)$ is systematic for mid-Z elements.

Relativistic, multiconfiguration calculations find that $R(3C/3D)$ decreases with higher atomic numbers, since the relative strength of the "forbidden" $3D$ line increases with respect to the $3C$ line as ions move away from LS-coupling and the contributions of different pure basis states to the physical upper level of each transition change. The strength of the forbidden line with respect to the resonance line increases as $\approx Z_c^6$ near LS-coupling, where Z_c is the effective ion charge. In the present work, we find that by making a small semiempirical correction to the multiconfiguration contribution to the strength of the $3D$ (increase) or $3C$ (decrease) line, we can improve the agreement between predicted and observed $R(3C/3D)$'s from an overprediction of $\gtrsim 20\%$ to $\approx 10\%$ for mid-Z ($Z=24$ to $Z=32$) elements. The magnitude of this configuration-interaction (CI) correction is determined by comparing energy-level calculations with high-precision measurements of energy differences between the upper levels of the $3C$ and $3D$ lines. In Sec. III of the present paper, we postulate how our semiempirical CI correction accounts for the infinite number of vanishingly small CI corrections to the strength of the $3C$ and $3D$ transitions.

In addition to the CI correction, we examine the effects of collisional-radiative (CR) processes on $R(3C/3D)$, namely collisional mixing of level populations and radiative cascades following electron-impact excitation. We show that in the coronal (low-density) limit, $R(3C/3D)$ is smaller than the ratio of collisional excitation rates which is often taken to obtain low-density line ratios, because radiative cascades preferentially enhance the population of the upper level of $3D$. At intermediate densities, $R(3C/3D)$ decreases due to collisional processes that tend to depopulate the upper level of $3C$ relative to that of $3D$, and then increases towards the

LTE (high-density) limit. By including both CI corrections and CR effects, the predicted values of $R(3C/3D)$ agree well with ratios measured for many elements in plasmas with a wide range of densities.

A recent paper [24,25] has proposed that the theoretical $R(3C/3D)$ can be brought into agreement with experiment by using large-scale, relativistic close coupling (CC) calculations of collision strengths, and demonstrated such agreement for Fe XVII. The present paper offers an alternative path for progress on improving modeled x-ray line ratios. We find that our CI correction to calculated collision strengths accounts for approximately half of the difference between the CC results in Refs. [24,25] and older distorted-wave approximation (DWA) calculations of $R(3C/3D)$. Radiative cascades (which were also included in [24,25]) contribute a correction of equal magnitude to the ratio and bring our DWA calculations into full agreement with experimental measurements; the present work thus offers a general path for the improvement of atomic structure codes and calls out the observation that a full treatment of CR processes is required even at low densities.

In Sec. II below, we present selected details of the HULLAC suite of codes [21] we use for atomic data generation. In Sec. III, we introduce our CI correction to calculations done with the HULLAC suite of codes for all elements from Cr ($Z=24$) to Ag ($Z=47$). The collisional-radiative model is introduced in Sec. IV, and CR effects on calculated values of $R(3C/3D)$ are shown over a wide range of electron densities. Evidence that these CI and CR corrections to calculated resonance to intercombination line ratios may be quite general is presented in Sec. V: We review published theoretical data sets for Fe XVII, showing that older calculations fail to predict $R(3C/3D)$ in the low-density limit and that their discrepancies are all in a direction consistent with the parameter that indicates the size of the needed CI correction. We also note that overpredictions of resonance to intercombination line ratios have been observed in He-like and Ni-like systems and show that the present approach may improve the agreement between experiment and theory in those systems as well. Finally, we conclude in Sec. VI.

II. CHOICE OF CODES

In the sections that follow, we present calculations for $R(3C/3D)$ from Ne-like ions of several elements for both low- and high-density plasmas. In every case, the data used to compute the ratio come from the HULLAC (version 7) suite of codes. Details on the codes in the HULLAC package are given in [21] and the references therein; here, we will only summarize the salient points. We choose to work with HULLAC data because the codes have been shown to be highly accurate [28–30] and easy to use for collisional radiative modeling [12,31,32]. We are highly familiar with the details of the HULLAC calculations and can assess the contributions of parts of the energy-level calculation to the derived energy eigenvalues.

Radial wave functions in HULLAC are computed with the RASER [33–35] code, which is a fully relativistic, multiconfiguration Dirac solver that operates in intermediate coupling. CI is allowed between all levels in the problem with common total angular momenta J and common parity, or between the levels of a set of user-specified configurations; for all calculations discussed here, we operated in the former manner. The atomic relativistic states are obtained from the many electron Dirac Hamilitonian that includes the Breit [36] interaction and quantum electrodynamic (QED) corrections. Wave functions for mixed-configuration states are found by diagonalizing a zeroth order Hamiltonian matrix that includes Dirac monoelectronic energies and the spherically averaged interaction between the electrons and a first-order perturbation that includes the nonspherical part of the electron-electron interaction; the results are mixed-configuration states, first-order energies and some correlation corrections. These correlation corrections are most important in the level energies of fairly low-Z members of the Ne-like isoelectronic sequence (Ti^{12+} and below) [37], and, since the shift in level energies has been found to be nearly uniform for all levels of a configuration [38], they cancel out of the energy difference between the upper levels of the $3C$ and $3D$ transitions and are not important to the present proposed CI correction.

Rather than use the variational principle that is the basis of the Hartree-Fock and Dirac-Fock methods of solution, RASER uses perturbation theory to minimize configuration-averaged energies using an analytic, parametric potential [34]. The single potential gives orthogonal wave functions, which are not guaranteed by the variational treatments. In the parametric potential, the exact exchange contribution to the first order energies is included without a need for an explicit exchange potential, and transition energies between nearby levels can be computed directly, rather than as the (small) differences between (large) total energies. For the present calculations, we minimized the energies of the $2s^22p^53\ell$ ($\ell \leqslant 2$) configurations in separate potentials for each ℓ value, and also used separate potentials to compute the wave functions and energies of levels in $2s^22p^6$, $2s^12p^63\ell$ ($\ell \leqslant 2$), $2s^22p^54\ell$ ($\ell \leqslant 3$), $2s^22p^5n\ell$ ($5 \leqslant n \leqslant 8, \ell \leqslant 4$), and $2s^12p^6n\ell$ ($4 \leqslant n \leqslant 8, \ell \leqslant 4$). Since the wave functions obtained using these separate potentials may not be orthogonal, RASER saves the optimized average energy for each configuration computed in its specified potential, then computes the energy of all fine-structure levels in the problem in a single specified potential (usually that of the ground configuration), thus insuring orthogonal wave functions. An energy shift is applied for the difference between the calculations in the optimal potential and the final potential, and all transition operators are evaluated with the orthogonal final-potential wave functions.

The contributions from the Breit operator are computed as a second-order perturbation with magnetic integrals according to the formalism of Grant (first paper of [35]) for averages of relativistic configurations. QED corrections (self-energy of a bound electron [39] and vacuum polarization [40]) are then added to the first-order energies by equating an effective nuclear charge for each bound electron to tabulated values [see Eq. (6) of [41]]. The set of configurations listed above generates 361 fine-structure levels; in the calculations investigating $R(3C/3D)$ for all elements from $Z=24$ to $Z=47$, we find accuracies in the absolute energies of the $3C$

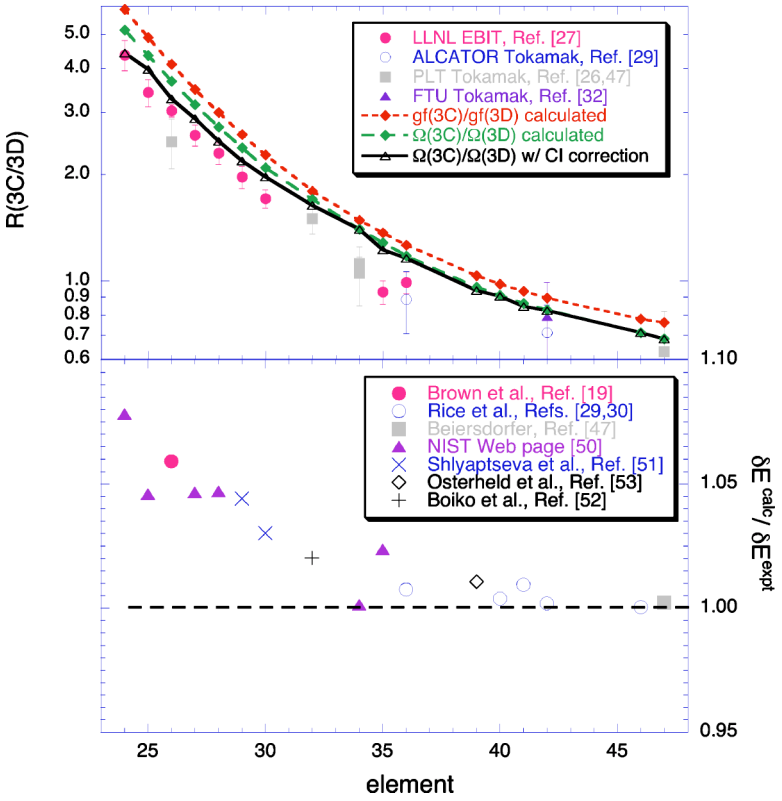

FIG. 1. (Color online) (Top) Summary of experimental 3*C* to 3*D* intensity ratios from low-density sources along with HULLAC calculations of the ratios of oscillator strengths (short dashes) and collision strengths (long dashes, with CI correction, solid line). (Bottom) The relative differences between calculated and measured 3*C* and 3*D* upper level energies.

and 3*D* levels compared to experimental measurements of between 1 part in 1500 to 1 part in 3300.

The piece of the HULLAC package that calculates the bound-bound electron-impact-excitation collision strengths is the COLEX suite of codes [42]. COLEX gets the transition energies and the relativistic wave functions from RASER and computes collision strengths semirelativistically in the distorted wave approximation (DWA) [43]. Here, semirelativistically means approximating the large radial component of the continuum-electron wave function with a Schrödinger solution and setting the small component to zero. Unlike the CC method, which couples open and closed channels, the DWA does not preserve unitarity. However, for highly charged ions such as those considered here, the actual collision-strength matrix elements are quite small, and the unitarization correction is not needed [44]. HULLAC achieves a great increase in the speed of the collision strength calculation by factoring the cross-section formulas into a radial part involving only one-electron wave functions and a sum over the partial waves of the continuum electron and an angular part involving the coupling between the bound electrons in the target states of each transition [42]. The latter piece is applicable to any coupling scheme and to mixed-configuration states. The exchange interaction between the continuum electron and the target states is kept, the effect being carried in values of the tensor rank for angular coefficients that might not satisfy the usual parity constraints for electric multipole transitions. The radial part of the calculation still depends on specific transitions through conservation of energy, i.e., $\Delta E_{if}=E_f-E_i=\varepsilon_{\text{in}}-\varepsilon_{\text{out}}$, where E is the energy of a target level, and ε is the energy of the incoming or outgoing continuum electron. However, instead of recomputing the radial integrals for each transition and each ε_{out}, it was found [42] that the radial integrals are smooth functions that can interpolated between a few values of ΔE_{if}. In particular, for a given ε_{out} and a given array of transitions, the integrals are calculated for the largest, smallest and mean transition energies, and linear interpolation on ΔE_{if} is used to estimate the rest [interpolation on $\log(\Delta E_{if})$ for dipole allowed integrals]. A great speedup of the calculation of the continuum orbitals has been achieved by an elaboration [45] of the classical phase amplitude description of the free-electron wave functions. The formula of Burgess [46] is used to estimate the sum over partial waves from some upper value to ∞; the upper value for each transition array is calculated in the COLEX suite by requiring that the estimated contribution from the high partial waves be small [21]. Given that high-Z ions can have configurations with enormous numbers of levels, and that the transition arrays coupling such configurations are also enormous, the factorization-interpolation method of the HULLAC suite can speed up calculations by orders of magnitude.

III. CI CORRECTIONS

Having described some details of the present calculations, we turn to a comparison of calculated line ratios to low-density experimental values. The state of this comparison for various elements is shown in Fig. 1. The dashed lines show the calculated ratios of oscillator strengths and electron-impact excitation collision strengths, as labeled, and the experimental ratios are taken from the literature [19,20,26,27,29,32,47]. For iron ($Z=26$), two experimental data points are given, one from an EBIT, which has a density

of $n_e \approx 10^{12}$ cm^{-3}, and one from the PLT tokamak, which has $n_e \approx 5\times 10^{13}$ cm^{-3}; both of these plasmas are near the low-density limit for $R(3C/3D)$. The EBIT value was observed from a nearly pure Fe^{16+} plasma while the tokamak value was observed with a line of sight that passed through a large range of plasma temperatures and included emission from several other iron ions, including Fe XVI lines. As was demonstrated by Brown *et al.* [20], the lower value of the tokamak ratio is due to a near coincidence between an inner-shell excited line of Fe XVI with the 3*D* line of Fe XVII. Data for Ge ($Z=32$), Se ($Z=34$), Kr ($Z=36$), Mo ($Z=42$), and Ag ($Z=47$) are also from tokamaks and may be similarly affected by lines from other ions; this possibility is reflected in their larger error bars.

The theoretical ratios of collision strengths given in Fig. 1 are close to line-intensity ratios in the low-density limit where collisional coupling and radiative cascades between levels in the Ne-like ion are neglected. In this limit, $R(3C/3D)$ is

$$I_{3C}/I_{3D} = \beta_{3C}Q_{3C}/\beta_{3D}Q_{3D}, \tag{1}$$

where β is the radiative branching ratio for the line in question (very near unity for 3*C* and 3*D* in all elements), and Q is the rate coefficient for impact excitation from the Ne-like ground state to the upper level of the transition. For the nearly monoenergetic electron beam of an EBIT, the rate coefficient is directly proportional to the collision cross section and the impact electron velocity: $Q=v_e\sigma(\varepsilon)$, where ε is the impact-electron energy. The cross section for excitation is related to the dimensionless collision strength by $\sigma=(Ry\pi a_0^2/g_0\varepsilon)\Omega$, where Ry is the Rydberg unit of energy, a_0 is the Bohr radius, and g_0 is the statistical weight of the initial level. Thus, for the EBIT observations, the $R(3C/3D)$ values are simply the ratios of any of the quantities Q, σ or Ω, and are identically given in Fig. 1, where we have calculated collision strengths at the electron beam energies reported for the EBIT experiments. We find that the ratio of $\Omega_{3C}(\varepsilon)$ to $\Omega_{3D}(\varepsilon)$ changes by less than 5% for Ne-like Fe when ε increases by two orders of magnitude from near the threshold energy for 3*C*, and by less than 2.5% for Ne-like Mo when ε increases by three orders of magnitude. For tokamaks, which have Maxwellian electron distributions characterized by an electron temperature T_e, collision rate coefficients $\langle v\sigma\rangle$ are obtained by averaging collision strengths over the electron distribution. This averaging introduces a factor of $\exp(-\Delta E_{ij}/T_e)$ to the rate coefficients. Since the ratio of the 3*C* to 3*D* collision strengths is nearly constant for impact-electron energies from threshold to tens of keV, the ratio of Maxwellian collision rates reduces to the ratio Ω_{3C}/Ω_{3D} and a factor $\exp(-\delta E/kT)$, where $\delta E=\Delta E(3C)-\Delta E(3D)$. The exponential factor is near unity for temperatures much larger than the energy difference δE, and for typical tokamak temperatures of 1–2 keV, the collision strength ratios given in Fig. 1 are within 5% of the Maxwellian-averaged collision rate ratios. Figure 1 shows that both EBIT and tokamak measurements of $R(3C/3D)$ are systematically overpredicted by about 20%.

In pure *LS* coupling, the 3*D* transition is strictly forbidden by both the ΔS and ΔL selection rules. The transition proceeds in intermediate coupling because the physical state of the upper level of the 3*D* transition contains admixtures from the upper levels of both 3*C* and 3*E* ($2p^6\,{}^1S_0$-$2p^5 3d^3P_1$). The increase of the 3*D* transition with larger atomic numbers is due to increasing relativistic effects in the upper level wave functions that move the system farther from *LS* coupling. Strength is transferred between upper levels of ionic transitions by configuration interaction, which takes place due to off-diagonal elements of the Coulomb interaction operator G. The strength of the interaction depends on the separation of the interacting levels. For some state ψ_1, to first order in the perturbation by the G operator, the mixed state reads

$$|\{\psi_1\}\rangle = |\psi_1\rangle + \sum_i |\psi_i\rangle\langle\psi_i|G|\psi_1\rangle/[E_1-E_i], \tag{2}$$

where the state in curly brackets is mixed, and the sum runs over all levels with the same parity and total angular momentum as $|\psi_1\rangle$. From Eq. (2), it is possible to deduce the strength of the transition from $|\{\psi_1\}\rangle$ to some level ψ_0 (mixed or pure) that is created by the interaction with basis states $|\psi_i\rangle$

$$S_{1,0} = \sum_i \sum_q \{\langle\psi_0|D_q^{(1)}|\psi_i\rangle\langle\psi_i|G|\psi_1\rangle/[E_1-E_i]\}^2, \tag{3}$$

where $\hat{D}=e\underline{r}$ is the electric dipole operator. Thus, the strength transferred to the transition $1\rightarrow 0$ by CI is proportional to the inverse square of the energy-level separation between level 1 and the perturbing level. (The case of level 0 being strongly mixed can be included too, such is not the case for the ground state of the Ne-like ions considered here.) Strong CI effects have been observed in the $n=3$ levels of higher-Z Ne-like ions when levels approach each other [48], and dramatic examples of the transfer of strength between nC and $n'D$ ($n>n'$) transitions in $n'>3$ levels have been documented when levels with different principal quantum numbers approach each other [28–30,49]. Since collision strengths are proportional to the transition strength in Eq. (3), the effect of CI on collision strengths manifests as the inverse square of the energy difference between the mixing levels. In our calculations, the upper levels of 3*C* and 3*D* are strongly mixed with each other for lower-Z elements (from Cr to Kr), and the upper level of 3*D* also mixes strongly with the upper level of 3*E* for all elements from Cr to Ag.

The convergence of the CI effect with increasing numbers of mixing levels is shown in Fig. 2 for the case of Fe XVII. In Fig. 2, we plot the calculated difference between the upper energy levels of the 3*C* and 3*D* transitions, δE^{calc}, relative to the difference measured by Brown *et al.*, δE^{expt}. Each point in the figure is calculated including another manifold of levels (all with principal quantum number n) to interact with all previously included levels: the circles are for calculations that are formed by the promotion of a single $n=2$ electron, the squares have configurations formed by promoting either one or two $n=2$ electrons. That is, the circle at $n=3$ includes interaction between all levels with a promotion of either a 2*s* or 2*p* electron to a 3ℓ ($\ell\leqslant 2$) orbital, and the square at $n=3$ includes those same singly excited configurations plus $2s^2 2p^4 3\ell 3\ell'$ and $2s^1 2p^5 3\ell 3\ell'$. Likewise, the circle at $n=4$

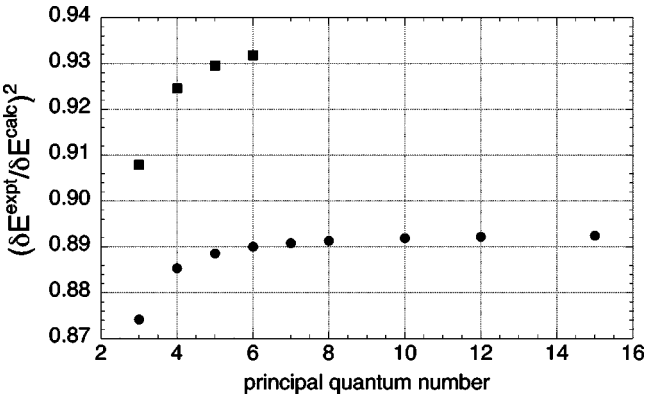

FIG. 2. Fe XVII $\delta E^{\mathrm{expt}}/\delta E^{\mathrm{calc}}$ versus highest principal quantum number included in the structure calculation. Circles: calculations with only singly excited levels; squares: with doubly excited levels included ($\delta E^{\mathrm{expt}}=13.365$ from Brown *et al.* [19]).

includes the $n=3$ configurations and all singly excited 4ℓ ($\ell\leqslant 3$) orbitals, and the square at $n=4$ includes all the singly and doubly excited $n=3$ configurations plus the singly excited $n=4$ configurations and $2s^2 2p^4 3\ell 4\ell'$ and $2s^1 2p^5 3\ell 4\ell'$ ($\ell'\leqslant 3$). For $n\geqslant 5$, only $n\ell$ orbitals with ($\ell\leqslant 4$) have been considered and for $n>8$, the $2sn\ell$ channels have been neglected. Beyond $n=6$, the doubly excited channels become too large to compute in an integrated fashion.

Figure 2 illustrates that the calculated value of δE^{calc} gets closer to the experimental value as the number of channels included in the CI correction increases (either by increasing the maximum value of n or by including doubly excited channels as well as singly excited channels). This decrease of δE^{calc} towards δE^{expt} is due to a much faster repulsion of the $3C$ upper level away from the continuum (towards $3D$) than for the upper level of $3D$. In the singly excited case, the actual change of the $3C$ level energy going from $n=3$ to $n\leqslant 15$ is ≈ 0.25 eV out of ≈ 826 eV, while the shift of the $3D$ level energy is only ≈ 0.095 eV out of ≈ 812 eV. The introduction of doubly excited configurations in the calculations is dramatic; their inclusion in just the $n=3$ case captures more of the correction required to get agreement with measure Fe XVII level energies than does going to $n\leqslant 15$ in the singly excited channel. The ratio of Ω_{3C}/Ω_{3D} is also affected by the limit of CI in the calculation. For the singly excited case, the Ω_{3C}/Ω_{3D} ratio goes from 3.85 ($n=3$ only) to 3.68 ($n\leqslant 8$, the value shown in Fig. 1), and is almost constant with n thereafter. Adding doubly excited levels with $n\leqslant 4$ (the largest model for which we could get COLEX to run), the Ω_{3C}/Ω_{3D} ratio decreases to 3.51.

The Fe XVII example above shows that the agreement of the calculated δE^{calc} with high-precision experimental measurements improves significantly when CI effects are explicitly included for a large number of states, and that better agreement in δE^{calc} leads to better agreement in Ω_{3C}/Ω_{3D}. These same observations obtain in all the Ne-like systems studied here. However, since the number of channels which can contribute to the CI effects on δE^{calc} is potentially infinite, we propose a semiempirical correction which can be used with calculations of any complexity. Following Eq. (3), the correction to $R(3C/3D)$ for the strength transferred by an infinite number of CI channels can be obtained by adjusting the dominant mixing in the upper levels of $3C$ (or $3D$) by the experimental energy separation of the interacting levels, giving

$$R(3C/3D)=\frac{\Omega_{3C}\beta_{3C}}{\Omega_{3D}\beta_{3D}}\left(\frac{\delta E^{\mathrm{expt}}}{\delta E^{\mathrm{calc}}}\right)^2. \tag{4}$$

As evidence for the general applicability of this formulation, we note that the two values of the Ω_{3C}/Ω_{3D} ratio quoted above (3.68 and 3.51) give nearly the same value (3.28 and 3.25) when the corrections from Fig. 2 are used. Therefore, throughout the remainder of this section and the next, we use calculations which include only CI contributions from singly excited states with $n\leqslant 8$.

The theoretical ratios of collision strengths given by the dashed line in Fig. 1 overestimate the experimental data points by an average of about 20% for $Z\leqslant 35$, falling well outside the experimental error bars. However, as shown in the bottom panel of Fig. 1, the HULLAC data also systematically overpredicts δE^{calc} in comparison to precise experimental measurements [19,30,50–54]. The intensity ratios given by the solid line in Fig. 1 are obtained by modifying the HULLAC intensity ratios according to Eq. (4). The corrected theoretical ratios are within about 10% of the experimental ratios. The CI correction is largest for $Z\leqslant 32$, where the system is far from both *LS* and *jj*-coupling and where the disagreement in $R(3C/3D)$ was greatest to begin with. The HULLAC predictions for the $3D$ level energy are less than 1 eV below the measured energies for $24\leqslant Z\leqslant 34$, while the predicted $3C$ level energies are $\lesssim 1$ eV larger than measured. For $Z>36$, the energies of both $3C$ and $3D$ are predicted to be 1–2 eV larger than observed. The opposite direction of the disagreements at the low-Z end of the range leads to the larger divergence between theory and observation seen in the lower panel of Fig. 1.

The magnitude of this CI effect, and the impracticality of including every important CI channel in *ab initio* calculations of energy levels, suggests that atomic-structure codes should have an option to converge their calculated energy levels to highly accurate spectroscopic measurements in order to improve atomic data for CR models. However, it is an open question whether the CI correction ought to be applied by increasing the rates into and out of the upper level of $3D$ or by decreasing those of $3C$. Either method will decrease $R(3C/3D)$, but the choice made here will affect other line ratios as well. Some guidance on this question is provided in [55], where several ratios of various $2p$-$3s$ and $2d$-$3d$ line intensities in the Fe XVII spectrum indicate that an overestimation of the $3C$ line intensity is the source of the disagreement between theory and experiment.

IV. CR CORRECTIONS AND DENSITY EFFECTS

Including CI corrections in the data is a necessary step towards reaching agreement with the experimental measurements, however, even with this correction, many theoretical points still fall outside the experimental error bars in Fig. 1. The intensity ratios given in Fig. 1 neglect radiative cascades and collisional processes, an approximation that is nearly

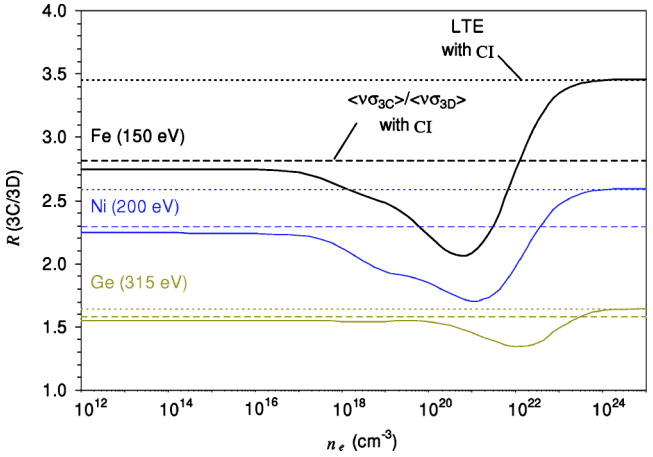

FIG. 3. (Color online) Density dependence of modeled $3C/3D$ intensity ratios for Fe, Ni, and Ge. The intensity ratios approach LTE limits (dotted) at high densities but deviate from ratios of collision rates (dashed) in the low-density limit due to radiative cascades.

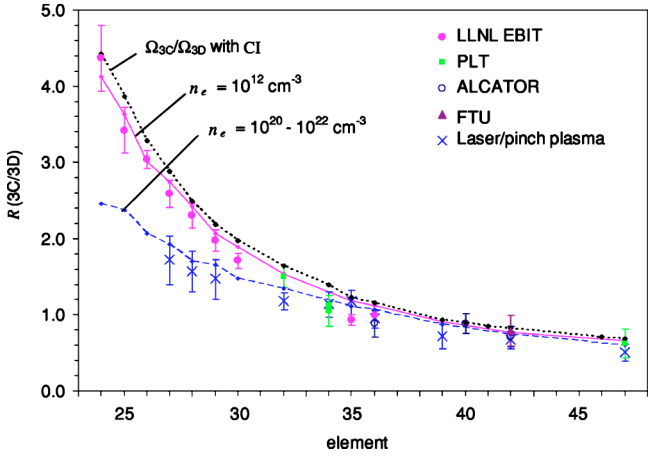

FIG. 4. (Color online) Experimental $R(3C/3D)$'s from low- and moderate-density sources with theoretical values. The low-density ratios were calculated using CI-corrected rates at beam energies 0.9–0.96 times the Ne-like ionization energy E_Z. The moderate-density values are from minima of curves like those given in Fig. 3 at temperatures 0.1–0.2 times E_Z.

ubiquitous in the literature. However, CR processes can affect line intensities even at low densities, particularly in closed-shell ions, where radiative cascades from excited levels that cannot decay directly to the ground state can feed into the upper levels of dipole-allowed lines. We have performed CR calculations using models based on HULLAC data to quantify the effects of CR processes on the $3C$ and $3D$ line intensities. The models include levels up to $n=8$ for Ne-like ions and up to $n=4$ (5) for F- (Na-) like ions. Selected autoionizing states with n up to 5 are included in the Na-like ions.

Figure 3 shows the results of these CR calculations for Fe, Ni, and Ge at Maxwellian temperatures from 0.1 to 0.2 times the ionization energy of the Ne-like ion. Ratios of the CI-corrected collisional rate coefficients (low-density limit) and ratios of radiative decay rates with Boltzmann factors (LTE/high-density limit) are given in Fig. 3 by dashed and dotted lines, respectively. Note that while the ratios reach the LTE limit at high densities, the ratios of collisional rates are about 5% larger than the intensity ratios found using a full CR treatment. This is because radiative cascades from high-n levels preferentially populate the upper level of $3D$ in $\Delta L=1$ transitions over the upper level of $3C$. The effects of cascades are largest for the low-Z models—decreasing $R(3C/3D)$ by almost 10% for Cr and only 3% for Mo—because the LS selection rules that govern radiative decay are most strict in low-Z systems. The effects of radiative cascades on $R(3C/3D)$ have been found to converge in the low-density limit when levels up to $n\approx 5$ are included in the CR models [56]. At intermediate densities, collisional processes (including ionization and recombination) tend to depopulate $3C$ preferentially over $3D$, and the intensity ratio falls further below the low- and high-density limits. The ratio reaches a minimum at some n_e which increases with Z, and then increases to its LTE limit at very high n_e.

With both the CR and the CI corrections, almost all of the calculated data points fall within the error bars of the low-density experimental data, as shown by the solid line in Fig. 4. Figure 4 also shows moderate-density ratios derived from published spectra from pinch and laser-produced plasmas [10,14,57–61]. The error bars on the moderate-density data points are large because of possible intensity contributions to $3C$ and $3D$ from F- and Na-like lines. In both density regimes, the calculated data agree well with experimental values. Both the CI and CR corrections to $R(3C/3D)$ are largest for smaller Z, where the deviation from experiment has historically been the most dramatic. For Z from 24 to 30 in particular, both inaccuracies in calculated level energies and significant CR effects conspire to invalidate simple ratios of *ab initio* collision strengths as predictors of $R(3C/3D)$.

V. DISCUSSION

In the preceding sections, we have shown how the combination of a semiempirical configuration-interaction correction and the inclusion of CR effects on line intensities can bring predicted values of $R(3C/3D)$ into agreement with experimental measurements over a wide range of electron densities across a significant swath of the neon isoelectronic sequence. In this section, we present evidence to show that such corrections may be very generally useful. First, we present a survey of $R(3C/3D)$ values obtained using published data for Fe XVII from a number of independent codes that treat CI in various levels of detail. We show that the deviation of the theoretical $R(3C/3D)$ values from experiment is strongly correlated with the deviation of δE^{calc} from δE^{expt}, and that applying the correction in Eq. (4) brings the theoretical ratios much closer to the experimental values. We then reprise overpredictions of resonance to intercombination line-intensity ratios which have been observed in other closed-shell ions, including He-, Mg-, and Ni-like ions, and discuss the possibility that corrections similar to those presented here for Ne-like ions may be applicable to other isoelectronic systems.

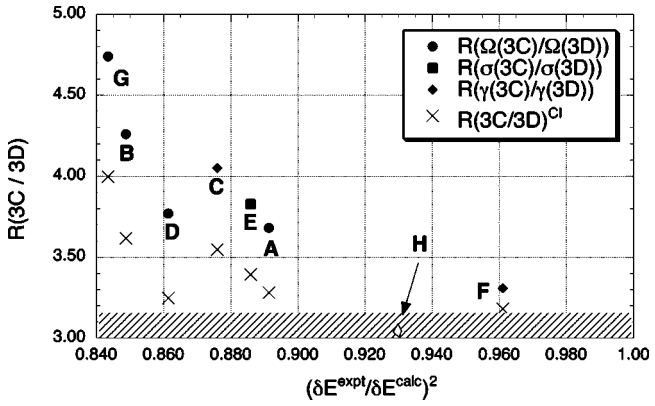

FIG. 5. Fe XVII $3C/3D$ ratios as predicted by various calculations: A (HULLAC, present work), B [62], C [63], D [64], E [65], F [66], G [67], and H [25]. The ratios including the CI correction [Eq. (4)] are given by the crosses. The measured value and the upper half of the uncertainty band reported by Brown *et al.* [19] are given by the shading at the bottom of the plot.

A. Review of other calculations

Figure 5 summarizes the predicted $3C/3D$ ratios for Fe XVII available from large, calculated data sets in the literature [28,25,62–68]. The ratios are plotted against $(\delta E^{\mathrm{expt}}/\delta E^{\mathrm{calc}})^2$ [i.e., the correction factor given in Eq. (4)]. Also shown in Fig. 5 is the *upper* half of the error band reported by Brown *et al.* for $R(3C/3D)$ from a low-density, optically thin, purely Fe^{16+} plasma in an EBIT, $R(3C/3D) = 3.04 \pm 0.12$. The ratios in Fig. 5 are computed taking the ratios of collision strengths (Ω): A (HULLAC, present work), B: (Cornille, Dubau and Jacquemot) [62], D: (Zhang and Sampson) [64], and G: (Bhatia, Feldman, and Seely) [67], cross sections (σ): E: (Hagelstein and Jung) [65], and rate coefficients or tabulated emissivities (γ): C: (Bhatia and Doschek) [63] at $T_e = 345$ eV, F: (Smith *et al.*) [66] at $T_e = 172$ eV, and H: (Chen *et al.*) [25] for $E_{\mathrm{beam}} = 1150$ eV. The tabulated emissivities of Bhatia and Doschek (C) include many of the CR corrections we discuss in Sec. IV and we have explicitly removed cascade contributions to the data of Smith *et al.* (F) [66]. We note that Waljeski *et al.* [18] give a calculated ratio of emissivities $R(\gamma(3C)/\gamma(3D)) = 3.8$ for T_e between 172 and 259 eV, based on a compilation of the other listed data sets, but since no calculated transition energies are given in [18], this point is not plotted in Fig. 5. Also left off the plot are published values of the ratio of collision strengths by Mohan [68], which had $\delta E^{\mathrm{calc}} \leqslant \delta E^{\mathrm{expt}}$ (thus the point would have been far to the right of 1.00 in Fig. 5), in spite of the fact that their $R(3C/3D) = 3.99$ value is consistent with the others shown. The same set of ratios is plotted chronologically in Ref. [15], along with two older calculations. Both of the older calculations [69,70] give $R(3C/3D)$ values that fall in the error band given by Brown *et al.* but do not give calculated transition energies. Generally, Fig. 5 shows that the calculations with larger discrepancies in the predicted $3C$ and $3D$ level separation also have $R(3C/3D)$ values that are farther away from the measured data.

We note that the calculations in [62,64,66,68] (points B, D, F, and the point from [68] not plotted) included interaction between singly excited $n=3$ and $n=4$ levels, and the calculations in [63,65,67] (points C, E, and G) only had $n=3$ levels. As indicated by the convergence study given in Fig. 2, all are deficient in accounting for CI effects on level energies. When the CI corrections given by Eq. (4) are included in the given data points, the calculated ratios fall much nearer the measured value (crosses in Fig. 5).

The data in Fig. 5 emphasize the motivation for this work: so far, calculations have been unable to provide consistent or reliable predictions for the optically thin value of this relatively simple line ratio. Figure 5 includes data from a wide variety of different calculations for (1) bound-state wave functions and (2) the collision strength of the bound-bound electron-impact excitations. The calculations of [68] (not plotted) used the CIV3 code [71] with orthogonal orbitals, and accounted for relativistic effects and *limited* CI (only with *LS* terms of $2s^2 2p^6$ and $2s^2 2p^5 3\ell$ configurations) at the first step, and then performed a CC calculation to obtain collision strengths. The works in Refs. [62] (B) and [63,67] (C and G) were performed with the SUPERSTRUCTURE code of Eissner [72]; wave functions were found from minimizing a nonrelativistic Hamiltonian with either a Thomas-Fermi-Dirac-Amaldi or a Thomas-Fermi potential, respectively, and relativistic effects were added later. In Ref. [62] (B), CI only from configurations of the form $2s^2 2p^6$ and $2s^2 2p^5 n\ell$ for $n \leqslant 4$) was allowed; in [67] (G) CI with only $2s^2 2p^5 3\ell$ was considered, while in [63] (C), $2s2p^6 3\ell$ configurations were added. DWA collision strengths, with various values of the highest-angular-momentum partial wave considered, were carried out in [62,63,67] (B, C, and G), and extrapolations beyond that cutoff value were considered for convergence. The calculations in [64] (D) are very similar to those done by the HULLAC package for both the bound wave functions and the collision strengths: a Dirac-Fock-Slater potential is minimized in solving the Dirac equation to find the bound wave functions; wave functions are automatically orthogonal, and the exchange potential is included from the beginning. The calculations are fully relativistic, and consider CI with all $n=3$ and $n=4$ levels formed from a single promotion of a $2s$ or $2p$ electron. The collision strengths in [64] are given by a relativistic DWA calculation that employs the same factorization technique originally developed for the HULLAC suite [42]. Finally, the calculations of [65] (E) provide relativistic DWA collision strengths. These calculations employ the YODA package, which uses relativistic Hartree-Fock orbitals to evaluate Coulomb and Breit terms [36] in the Hamiltonian, as well as self-energy and vacuum polarization. A finite-sized atomic nucleus is considered with a Fermi charge distribution. Continuum orbitals for the collision strength calculation are computed in the DWA, neglecting exchange with bound-state orbitals.

Thus, a wide range of codes that employ a wide range of techniques and approximations have been used to compute the ratio $R(3C/3D)$, and in each case, the calculated ratios can be reduced towards the experimental value by applying our proposed semiempirical correction. (The special case of point "H" will be discussed further below.) Note that even with the imposed CI correction, the crosses shown in Fig. 5 still lay outside the error band of the Brown *et al.* measurement, indicating that the further correction to the ratio due to

CR effects is required. [If one uses the ratio of collision rates at $T_e = 172$ eV in [66] that includes the effect of cascades, one finds a ratio $R(3C/3D) = 3.08$ that falls within the error band in Fig. 5 without modification.]

Special discussion must be given to the recent calculations of Chen, Pradhan, and Eissner [24,25]. Extensive CC calculations for all the collision strengths among the 89 fine-structure levels (generated by configurations of the form $2s^2 2p^6$, $2\ell^7 3\ell'$, and $2\ell^7 4\ell'$), have been applied in a collisional radiative model to calculate $R(3C/3D)$ and $R(3E/3D)$ line-intensity ratios. The CI contributions to the CC collision strength calculations in [24,25] are much more extensive than those of both the CC calculations of [68] and the DWA calculations in [62,63,67]. The atomic-structure calculations in [24,25] are done with radial functions from SUPERSTRUCTURE that are used to find fine-structure level energies from the Breit-Pauli Hamiltonian [73]. The $3C$ and $3D$ upper level energies that come out of this are very close to the measured value, with $\delta E^{\mathrm{calc}} = 13.874$ eV (versus $\delta E^{\mathrm{expt}} = 13.365$ eV). A Breit-Pauli R-matrix code [74] is used to compute the CC collision strengths in a manner that accounts for the N-shell ($n=4$) contribution to resonance structure. Taking a Gaussian average over resonance structures in the data of [25], which approximates the physical spread in the electron beam energies in Ref. [19], the authors find a value of $R(\gamma(3C)/\gamma(3D)) = 3.10$ at an energy ≈ 324 eV above the threshold for the $3C$ transition. We have shown above that a semiempirical accounting for the infinite spectrum of CI corrections to the calculated collision strengths, which arise from singly excited Ne-like levels from higher-n configurations, and, primarily, from doubly excited Ne-like configurations, has approximately the same effect on $R(3C/3D)$ as the spectrum of resonances in Ref. [25].

B. Other closed-shell ions

The Ne-like systems investigated in this paper are not the only closed-shell ions for which overpredictions of resonance-to-intercombination line ratios have been observed. A previous work has noted difficulty in predicting the resonance to intercombination line-intensity ratio in $\Delta n = 0$ transitions in Mg-like ions for almost the same range of elements looked at here [75]; there, an appeal to an unlikely departure from ionization equilibrium was needed to bring models into agreement with observations.

In 2000, a survey [76] of low-density measurements on the Livermore EBIT of $n = 3 \rightarrow 1$ line ratios in He-like systems with Z from 12 to 26 showed that the resonance line $(1s3p\ ^1P_1\text{-}1s^2\ ^1S_0)$ to intercombination line $(1s3p\ ^3P_1\text{-}1s^2\ ^1S_0)$ ratio was systematically overpredicted by both HULLAC and MCDF [77] codes. Although no high-precision transition energy measurements were given in [76], we have compared reference data from [50] to data calculated using the FAC code [22] for several He-like ions and have found that the calculated energy difference between the upper levels of the resonance and intercombination lines is larger than the reference energy difference. Including the implied CI correction in a manner analogous to Eq. (4) would decrease the theoretical He-like resonance to intercombination line-intensity ratios given in [76], bringing them closer to the measured ratios. We note that the experiment in [76] was designed to prevent excitation into He-like states with $n \leqslant 4$ in order to minimize the effects of radiative cascades on the measured line intensities (such flexibility is one of the great advantages of EBIT measurements); however, preliminary CR calculations suggest that collisional interactions may still play a role in the He-like line formation processes.

More recently, high-precision measurements of Ni-like Au [78] and W [79] spectra have been performed on the Livermore EBIT. The Ni-like ion has a ground state configuration of $3s^2 3p^6 3d^{10}\ ^1S_0$ and strong excitation channels from that ground state to the $3d^9 4f\ ^1P_1$ (resonance) and $3d^9 4f\ ^3P_1$ (intercombination) states. Although analysis of the Ni-like systems is not as well developed as that of the He- and Ne-like systems discussed above, in this case, too, the resonance to intercombination line ratios appear to be overpredicted by theoretical calculations. For both Ni-like Au and Ni-like W, the theoretical energy differences between the upper levels of the resonance and intercombination transitions deviates from the experimental δE in the direction that would reduce the theoretical ratio when applying the CI correction of Eq. (4). A preliminary model of the Ni-like Au system based on HULLAC data predicts that the CI correction would reduce the theoretical line ratio by about 13%, and that CR effects included using the CR model would decrease the calculated ratio by another 5%. The two corrections would bring the calculated ratio into reasonable agreement with the measured value. Further study of the He-like and Ni-like systems may help resolve the question of how best to implement the proposed CI corrections in large data sets used for collisional-radiative modeling.

VI. CONCLUSION

We have shown that theoretical predictions of the Ne-like $3C/3D$ line-intensity ratio can be brought into agreement with experimental data across a wide range of electron densities by including a semiempirical configuration-interaction correction and collisional-radiative effects, thus resolving a significant overprediction that has been troublesome for decades. We have shown that the semiempirical correction can be used to bring calculations of $R(3C/3D)$ in Fe XVII from a wide variety of codes much closer to agreement with high-precision low-density measurements, and have pointed to evidence that similar CI corrections and CR effects may also be important in describing resonance-to-intercombination line ratios in Ni- and He-like ions. These results should point the way for development of robust spectroscopic plasma diagnostics in both astrophysical and laboratory plasmas.

ACKNOWLEDGMENTS

This work was performed under the auspices of the U.S. Department of Energy by University of California Lawrence Livermore National Laboratory under Contract No. W-7405-Eng-48.

[1] R. L. Blake, T. A. Chubb, H. Friedman, and A. E. Unzicker, Astrophys. J. **142**, 1 (1965).
[2] J. H. Parkinson, Sol. Phys. **42**, 183 (1975).
[3] R. H. Hutcheon, F. P. Pye, and K. D. Evans, Mon. Not. R. Astron. Soc. **175**, 489 (1976).
[4] K. J. H. Phillips *et al.*, Astrophys. J. **256**, 774 (1982).
[5] H. R. Rugge and D. L. McKenzie, Astrophys. J. **297**, 338 (1985).
[6] C. R. Canizares *et al.*, Astrophys. J. Lett. **539**, L41 (2000).
[7] A. C. Brinkman *et al.*, Astrophys. J. Lett. **530**, L111 (2000).
[8] R. Mewe, A. J. J. Raassen, J. J. Drake, J. S. Kaastra, R. L. J. van der Meer, and D. Porquet, Astron. Astrophys. **368**, 888 (2001).
[9] C. W. Mauche, D. A. Liedahl, and K. B. Fournier, Astrophys. J. **560**, 992 (2001).
[10] W. H. Goldstein, R. S. Walling, J. Bailey, M. H. Chen, R. Fortner, M. Klapisch, T. Phillips, and R. E. Stewart, Phys. Rev. Lett. **58**, 2300 (1987).
[11] B. K. F. Young, B. G. Wilson, D. F. Price, and R. E. Stewart, Phys. Rev. E **58**, 4929 (1998).
[12] S. B. Hansen *et al.*, Phys. Rev. E **66**, 046412 (2002).
[13] A. S. Shlyaptseva *et al.*, Phys. Rev. E **67**, 026409 (2003).
[14] S. B. Hansen *et al.*, Phys. Rev. E **70**, 026402 (2004).
[15] P. Beiersdorfer, Annu. Rev. Astron. Astrophys. **41**, 343 (2003).
[16] J. L. R. Saba, J. T. Schmelz, A. K. Bhatia, and K. T. Strong, Astrophys. J. **510**, 1064 (1999).
[17] J. T. Schmelz, J. L. R. Saba, J. C. Chauvin, and K. T. Strong, Astrophys. J. **477**, 509 (1997).
[18] K. Waljeski *et al.*, Astrophys. J. **429**, 909 (1994).
[19] G. V. Brown, P. Beiersdorfer, D. A. Liedahl, K. Widmann, and S. M. Kahn, Astrophys. J. **502**, 1015 (1998).
[20] G. V. Brown, P. Beiersdorfer, H. Chen, M. H. Chen, and K. J. Reed, Astrophys. J. Lett. **557**, L75 (2001).
[21] A. Bar-Shalom, M. Klapisch, and J. Oreg, J. Quant. Spectrosc. Radiat. Transf. **71**, 169 (2001).
[22] M. F. Gu, Astrophys. J. **590**, 1131 (2003); **582**, 1241 (2003).
[23] H. L. Zhang and D. H. Sampson, At. Data Nucl. Data Tables **37**, 17 (1987).
[24] G. X. Chen and A. K. Pradhan, Phys. Rev. Lett. **89**, 013202 (2002).
[25] G. X. Chen, A. K. Pradhan, and W. Eissner, J. Phys. B **36**, 453 (2003).
[26] P. Beiersdorfer, S. von Goeler, M. Bitter, and D. B. Thorn, Phys. Rev. A **64**, 032705 (2001).
[27] G. V. Brown, P. Beiersdorfer, and K. Widmann, Phys. Rev. A **63**, 032719 (2001).
[28] K. B. Fournier *et al.*, J. Quant. Spectrosc. Radiat. Transf. **81**, 167 (2003).
[29] J. E. Rice, K. B. Fournier, J. A. Goetz, E. S. Marmer, and J. L. Terry, J. Phys. B **33**, 5435 (2000); J. E. Rice (private communication).
[30] J. E. Rice *et al.*, Phys. Rev. A **53**, 3953 (1996).
[31] K. B. Fournier *et al.*, Phys. Rev. E **67**, 016402 (2003).
[32] K. B. Fournier, W. H. Goldstein, D. Pacella, R. Bartiromo, M. Finkenthal, and M. May, Phys. Rev. E **53**, 1084 (1996).
[33] M. Klapisch, Comput. Phys. Commun. **2**, 239 (1971).
[34] M. Klapisch, J. L. Schwob, B. S. Fraenkel, and J. Oreg, J. Opt. Soc. Am. **67**, 148 (1977).
[35] I. P. Grant, Adv. Phys. **19**, 747 (1970); J. Phys. B **7**, 1458 (1974).
[36] G. Breit, Phys. Rev. **34**, 553 (1929); **36**, 383 (1930); **39**, 616 (1932); I. P. Grant and N. C. Pyper, J. Phys. B **9**, 761 (1976).
[37] J. A. Cogordan, S. Lunell, C. Jupén, and U. Litzén, Phys. Scr. **31**, 545 (1985).
[38] J. A. Cogordan and S. Lunell, Phys. Scr. **33**, 406 (1986).
[39] G. W. Erickson, J. Phys. Chem. Ref. Data **6**, 831 (1977).
[40] P. J. Mohr, Phys. Rev. A **26**, 2338 (1982); Phys. Rev. Lett. **34**, 1050 (1975); Ann. Phys. (N.Y.) **88**, 53 (1974).
[41] K. B. Fournier, At. Data Nucl. Data Tables **68**, 1 (1998).
[42] A. Bar-Shalom, M. Klapisch, and J. Oreg, Phys. Rev. A **38**, 1773 (1988).
[43] M. S. Pindzola, A. K. Bhatia, and A. Temkin, Phys. Rev. A **15**, 35 (1977).
[44] P. L. Hagelstein, Phys. Rev. A **34**, 874 (1986).
[45] A. Bar-Shalom, M. Klapisch, and J. Oreg, Comput. Phys. Commun. **93**, 21 (1996).
[46] A. Burgess, J. Phys. B **7**, L364 (1974).
[47] P. Beiersdorfer, Ph.D. thesis, Princeton University, 1988.
[48] N. Nakamura, D. Kato, and S. Ohtani, Phys. Rev. A **61**, 052510 (2000).
[49] E. Biémont *et al.*, J. Phys. B **33**, 2153 (2000).
[50] http://physics.nist.gov/cgi-bin/AtData/main_asd
[51] A. Shlyaptseva *et al.*, Phys. Scr. **52**, 377 (1995).
[52] V. A. Boiko, A. Ya. Faenov, and S. A. Pikuz, J. Quant. Spectrosc. Radiat. Transf. **19**, 11 (1994).
[53] A. L. Osterheld, J. Nilsen, S. Y. Khakhalin, A. Y. Faenov, and S. A. Pikuz, Phys. Scr. **54**, 240 (1996).
[54] P. Beiersdorfer *et al.*, Phys. Rev. A **34**, 1297 (1986).
[55] P. Beiersdorfer, M. Bitter, S. von Goeler, and K. W. Hill, Astrophys. J. **610**, 616 (2004).
[56] S. B. Hansen, Ph.D. thesis, University of Nevada, Reno, 2003.
[57] O. Peyrusse *et al.*, J. Appl. Phys. **65**, 3802 (1989).
[58] J. Bailey *et al.*, J. Phys. B **19**, 2639 (1986).
[59] P. G. Burkhalter, J. Shiloh, A. Fisher, and R. D. Cowan, J. Appl. Phys. **50**, 4532 (1979).
[60] B. K. F. Young *et al.*, J. Quant. Spectrosc. Radiat. Transf. **51**, 417 (1994).
[61] B. K. F. Young *et al.*, Phys. Rev. Lett. **62**, 1266 (1989).
[62] M. Cornille, J. Dubau, and S. Jacquemot, At. Data Nucl. Data Tables **58**, 1 (1994).
[63] A. K. Bhatia and G. A. Doschek, At. Data Nucl. Data Tables **52**, 1 (1992).
[64] H. L. Zhang and D. H. Sampson, At. Data Nucl. Data Tables **43**, 1 (1989).
[65] P. L. Hagelstein and R. K. Jung, At. Data Nucl. Data Tables **37**, 121 (1987).
[66] B. W. Smith, J. C. Raymond, J. B. Mann, and R. C. Cowan, Astrophys. J. **298**, 898 (1985).
[67] A. K. Bhatia, U. Feldman, and J. F. Seely, At. Data Nucl. Data Tables **32**, 435 (1985).
[68] M. Mohan, R. Sharma, and W. Eissner, Astrophys. J., Suppl. Ser. **108**, 389 (1997).
[69] J. B. Mann, At. Data Nucl. Data Tables **29**, 407 (1983).
[70] O. Bely and F. Bely, Sol. Phys. **2**, 285 (1967).
[71] A. Hibbert, Comput. Phys. Commun. **9**, 141 (1975).
[72] W. Eissner, M. Jones, and H. Nussbaumer, Comput. Phys. Commun. **8**, 270 (1974).
[73] K. A. Berrington, W. B. Eissner, and P. H. Norrington, Comput. Phys. Commun. **92**, 290 (1995).
[74] N. S. Scott and K. T. Taylor, Comput. Phys. Commun. **25**, 347

(1982).
[75] K. B. Fournier, W. H. Goldstein, M. Finkenthal, R. E. Bell, and J. L. Terry, J. Electron Spectrosc. Relat. Phenom. **80**, 283 (1996).
[76] A. J. Smith *et al.*, Phys. Rev. A **62**, 012704 (2000).
[77] M. H. Chen, Phys. Rev. A **31**, 1449 (1985); **33**, 994 (1986).
[78] M. J. May, K. B. Fournier, P. Beiersdorfer, H. Chen, and K. L. Wong, Phys. Rev. E **68**, 036402 (2003).
[79] P. Neill *et al.*, Can. J. Phys. **82**, 931 (2004).